CHAPTER 3

MATERIALS AND METHODS

3. Materials and Methods

3.1 Materials

3.1.1 Chemicals used

Table 3.3 lists the various compounds utilised during the experimental activity.

3.1.2 Composition of Testing Material

The corrosion tests were performed on N80 steel and mild steel. The composition of N80 used in Chapter 4 section 4.1,4.2, and 4.3 has following composition (wt. %).

Table 3.1 Composition of N80 steel (wt. %)

C	Mn	P	Si	S	Cr	Fe
0.31	0.92	0.010	0.19	0.008	0.2	Balance

Whereas the composition of mild steel used in Chapter 4 section 4.4 is given in Table 3.2 with the composition in wt. %.

Table 3.2 Composition of mild steel (wt. %).

C	Mn	P	Si	S	Fe
0.17	0.37	0.010	0.20	0.03	Balance

3.1.3. Test specimen for electrochemical study

N-80 steel strips of the above composition having a working area of 1 cm^2 were used for all electrochemical studies.

3.1.4. Test solutions.

As corrosive media, HCl solutions of the appropriate concentrations were utilised. All of the test solutions were prepared using doubly distilled water.

3.1.5. Inhibitors used.

10 inhibitors were used in the present study. Some inhibitors such as Substituted Triazine, Chromeno Naphthyridines, Hydroxy quinoline derivatives, and substituted Benzimidazole were synthesized in the laboratory. They are listed below:

(A) Substituted Triazines

(1) 1,3,5-triphenyl-1,3,5-triazinane. (TZ-1)

(2) 1,3,5-tris(4-nitrophenyl)-1,3,5-triazinane. (TZ-2)

(3) 1,3,5-tris(4-methoxyphenyl)-1,3,5-triazine. (TZ-3)

(B) Chromeno Naphthyridiens.

(1) 5-amino-9-hydroxy-2phenyl1-11b dihydrochromeno (4,3,2-de) (1,6 naphthyridine) 4- carbonitrile. (CN-1)

(2) 5-amino- 9-hydroxy-2-(4methoxy phenyl) 1-11b dihydrochromeno (4,3,2 -de) (1,6 naphthtyridine) 4-carbonitrile. (CN-2)

(3) 5-amino- 9-hydroxy-2-styril 1-11b dihydro 7-oxa 3,6 diazabenzo (de) anthracene 4-carbonitrile. (CN-3)

(C) Quinolines derivatives

(1) 2-amino-7-hydroxy-4-phenyl-1,4-dihydroquinoline-3-carbonitrile - (AHQ-1).

(2) 2-amino-7-hydroxy-4(4methoxyphenyl)1,4-dihydroquinoline-3-carbonitrile- -(AHQ-2)

(3) 2-amino-7-hydroxy-4(4styryl)1,4-dihydroquinoline-3-carbonitrile -(AHQ-3).

(D) Benzimidazoles.

(1) 2-styryl-*1H*-benzimidazole. -(STBim)

Table 3.3 Name, Molecular formula, and Purity of Chemicals used.

Name	Mol. formula	Make	% Purity
Formaldehyde (40%)	HCHO	Spectrochem	98-100
Aniline	C_6H_7N	Avra	99
Paranitro aniline	$C_4H_6N_2O_2$	Avra	98.5-100
Paramethoxy aniline	$C_7H_9NO_2$	Avra	98.5-100
Ethanol	C_2H_6O	Spectrochem	99
Malononitrile	$C_3H_2N_2$	Merck	98-100
2,4 dihydroxyacetophenone	$C_8H_8O_3$	Himedia	98-100
Benzaldehyde	C_7H_6O	Himedia	99-100
Anisaldehyde	$C_8H_8O_2$	Himedia	99-100
Cinnamaldehyde	$C_9H_8O_1$	Himedia	99-100
Silica –gel	-	Merck	-
Ammonium acetate	$C_2H_8NO_2$	Qualigens	99.5
Ethylacetoacetate	$C_6H_{10}O_3$	Himedia	99.5
Orthophenylene diamine	$C_6H_8N_2$	Merck	90
Boric acid	$C_6H_7N_3O$	Himedia	99.5
Hydrochloric Acid (35%)	HCl	Merck	99
Resorcinol	$C_6H_6O_2$	Sigma	98

3.1.5.1. Synthesis of Substituted Triazines [(Singh, Shukla, and Quraishi 2011)]

A beaker containing a mixture of aryl amines (0.01mol) and 37% HCHO solution (0.01mol) was introduced for ultrasonication containing a mixture of ethanol and water (60: 40). After completion the of reaction (as monitored by TLC), the product was filtered and washed several times with ethanol. synthesis of Substituted Triazines is shown in the scheme 3.1.

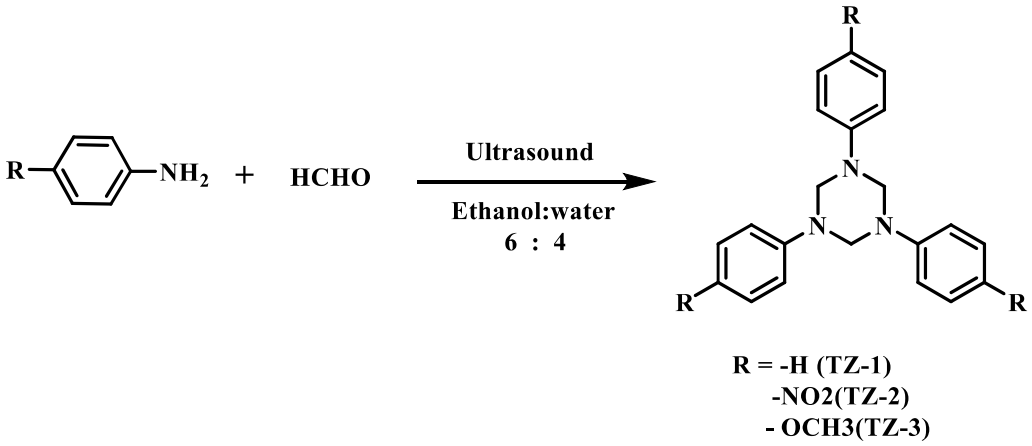

Scheme 3.1 Synthesis of Substituted Triazines.

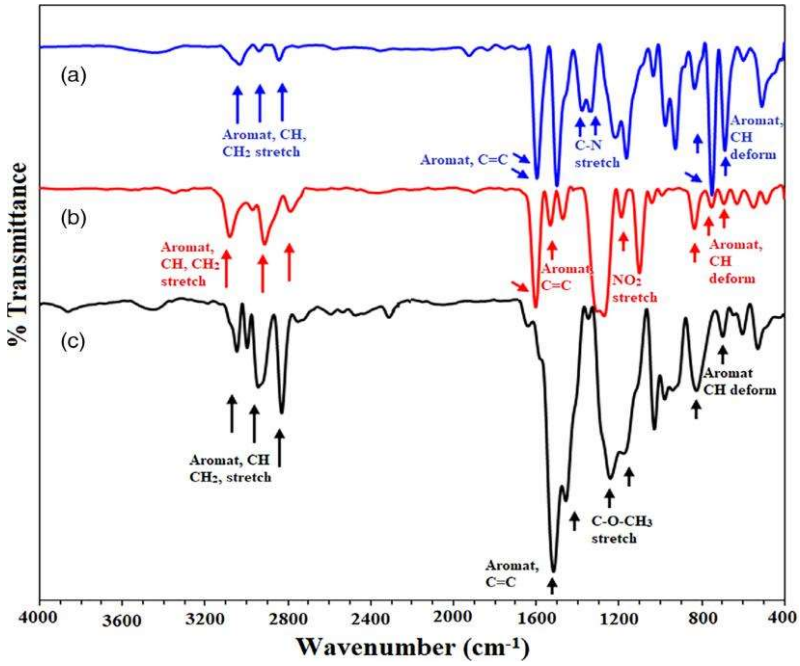

Figure 3.1 FTIR spectra of synthesized Triazine derivatives.

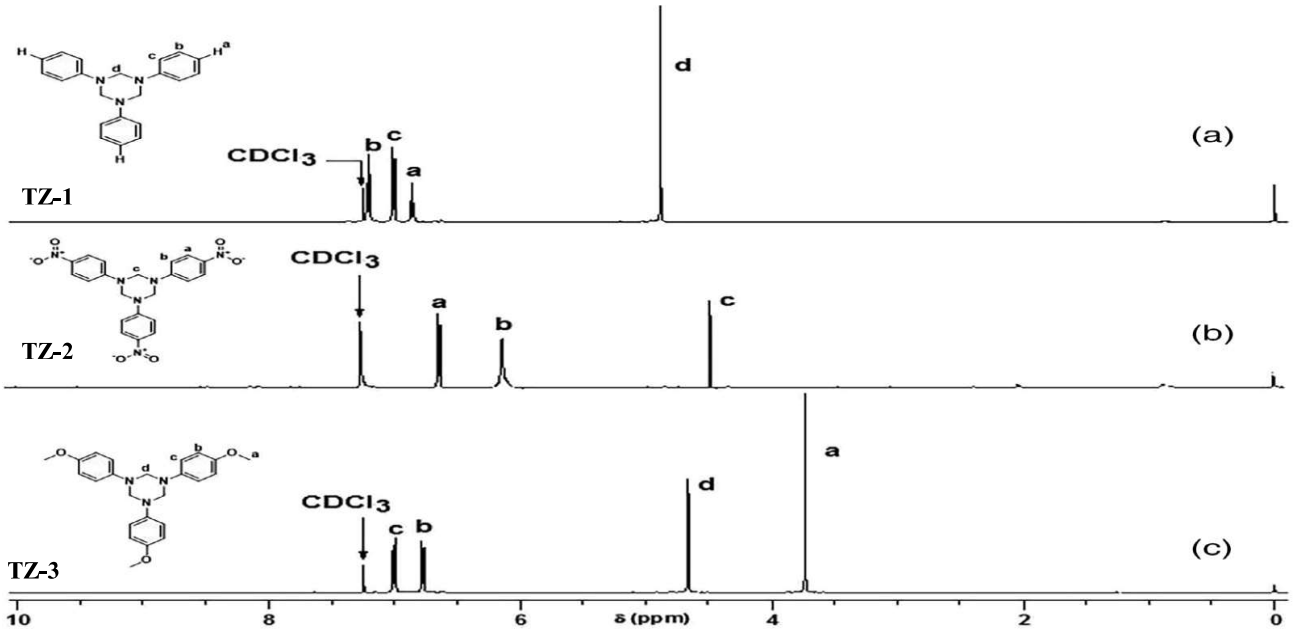

Figure 3.2 ^{1}H-NMR spectra of synthesized Triazine derivatives.

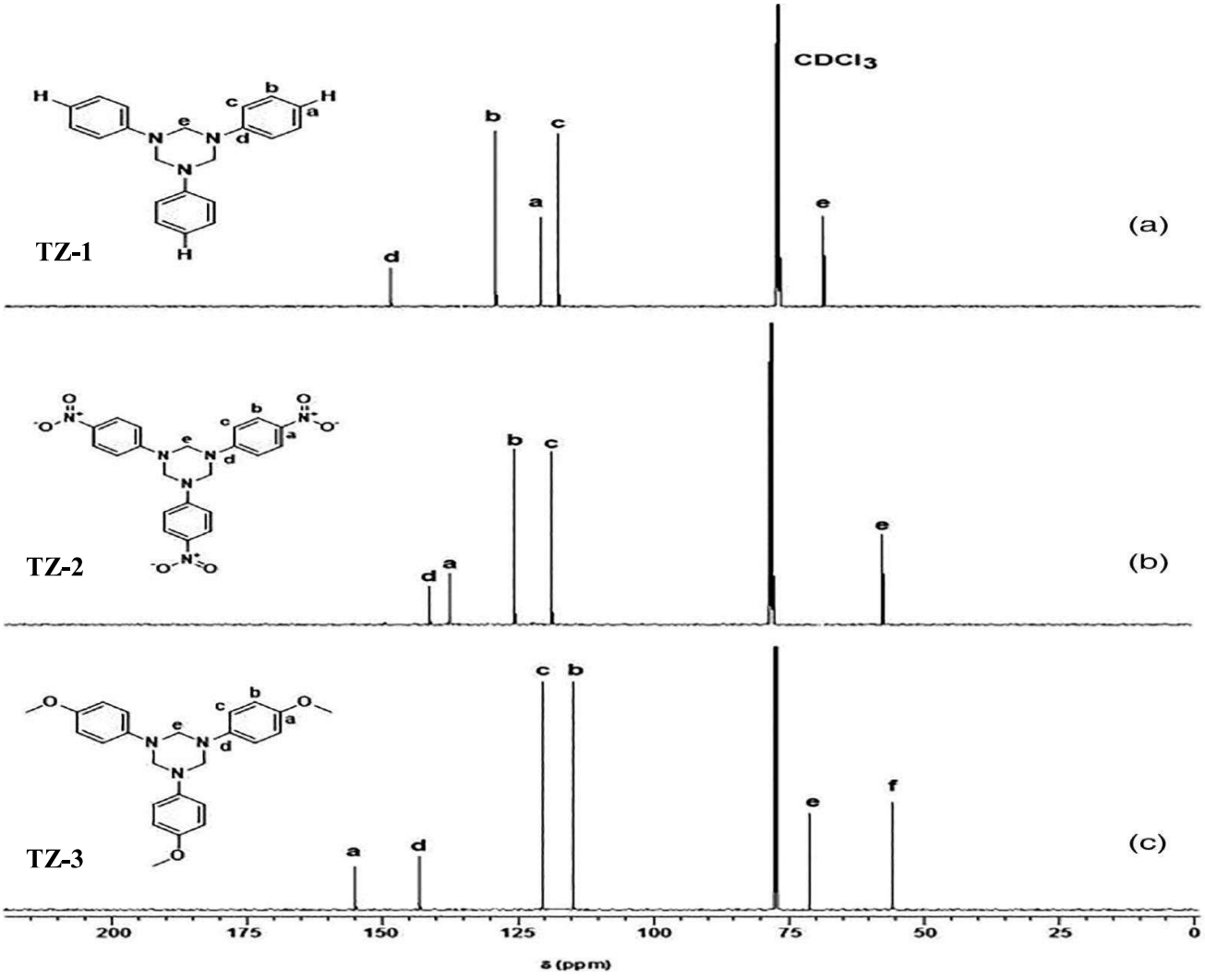

Figure 3.3 ^{13}C-NMR spectra of synthesized Triazine derivatives.

Table 3.4 The name, structure and characterization data of Substituted Triazines based inhibitors.

S. No.	Name and Abbreviation of Inhibitor	Inhibitor structure	Characterization data
1.	1,3,5-triphenyl-1,3,5-Triazine. **(TZ-1)**	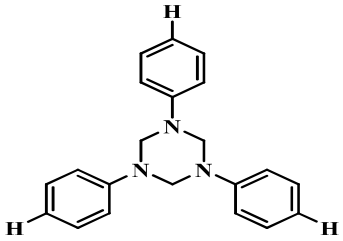	$C_{21}H_{21}N_3$ (mol. wt.315.42) (M.P. 137-140^{0}C) **FTIR** (Vmax/ cm^{-1}) (KBr): 3031 (CH str.), 2937 (CH_2 str.), 2841 (CH_2 str.), 1594, 1497 (aromatic ring str.), 1376, 1335 (amines CN str.), 1216, 1162, 1032, 974, 926 (aromatic CH bend), 833, 748. **^{1}H NMR** (400 MHz) ($CDCl_3$) δ (ppm): 4.88 (6H, s), 6.86 (3H, t), 7.01 (6H, d), 7.21 (6H, t). **^{13}C NMR** ($CDCl_3$) δ (ppm): 68.55 (3C),117.66 (6C), 120.90 (3C), 129.15 (6C), 148.60 (3C).
2.	1,3,5-tris (4-nitrophenyl)-1,3,5-Triazine. **(TZ-2)**	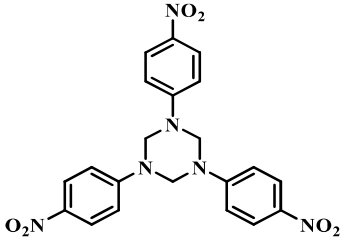	$C_{21}H_{18}N_6O_6$ (mol. wt.450.41). (M.P. 284-288^{0}C); **FTIR** (Vmax/ cm^{-1}) (KBr): 3044(aromatic CH), 2827(alkane CH_3, CH_2) 655 (C–S–C), 2835 (C–H), 1120 (C–C),1355 (amines CN str.), 824 (C-O-C symmetric), **^{1}H NMR** (400 MHz) = ($CDCl_3$) δ (ppm): 3.74 (9H, s), 4.67 (6H, s), 6.77 (6H, d), 7.01 (6H, d). 4.49 (6H, s), 6.13 (6H, d), 6.64 (6H, d). **^{13}C NMR** ($CDCl_3$) δ (ppm): 55.48 (3C), 71.10 (3C), 114.39 (6C), 120.03 (6C), 142.58 (3C), 154.43 (3C).

3.	1,3,5-tris (4-me thoxyphenyl)-1,3,5-Triazine **(TZ-3)**	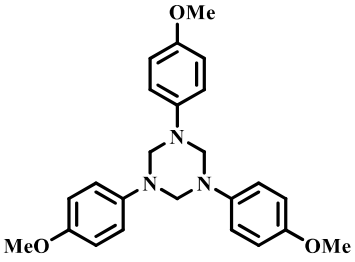	$C_{24}H_{27}N_3O_3$ (mol. wt.405.50). (M.P. 126-130^{0}C); **FTIR** (Vmax/ cm^{-1}) (KBr): 3044 (aromatic CH str.), 2994, 2940 (alkane CH_3, CH_2asymmetricstr.), 1514 (aromatic ring str.),1355 (amines CN str.), 1240, 1191(C-O-C asymmetric str.),1191 (C-O-C symmetric str.), 977, 930 (aromatic CH bend) cm^{-1}. **^{1}H NMR** (400 MHz) ($CDCl_3$) δ (ppm): 3.74 (9H, s), 4.67 (6H, s), 6.77 (6H, d), 7.01 (6H, d).4.49 (6H, s), 6.13 (6H, d), 6.64 (6H, d). **^{13}C NMR** ($CDCl_3$) δ(ppm): 55.48 (3C), 71.10 (3C), 114.39 (6C), 120.03 (6C),

3.1.5.2. Synthesis of Chromeno naphthyridines [(Wu et al. 2010)]

Malononitrile(4mmol) in 100 mL and Aromatic aldehyde (2mmol) in 50 mL were mixed and stirred on a magnetic stirrer for 15 minutes and 2,4 dihydroxyacetophenone (2mmol) and silica gel (0.03g) were dissolved in the beaker of 100 mL containing 10 mL of water. Finally, both solutions mixed with each other. They stirred for 2 hours at 80^{0}C temperature. After completion of the reaction, the compounds were recrystallized from ethanol. The outline for the synthesis of Chromeno naphthyridines is shown in scheme- 3.2.

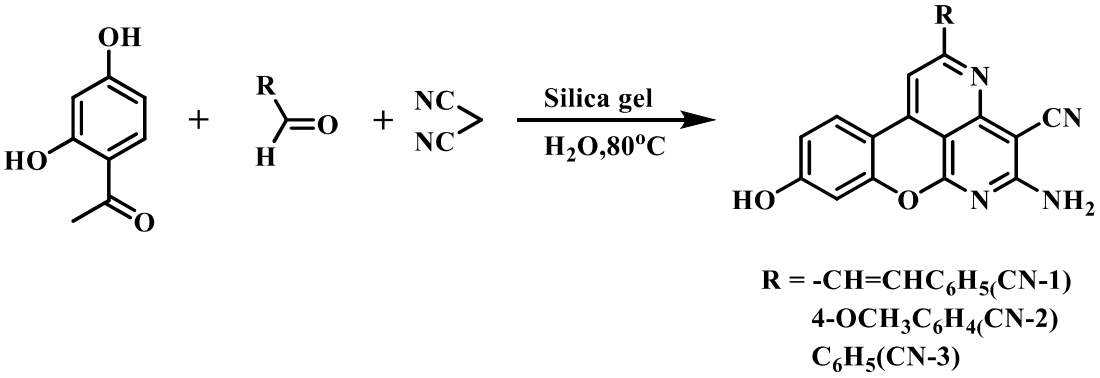

Scheme 3.2 Synthesis of Chromeno naphthyridines

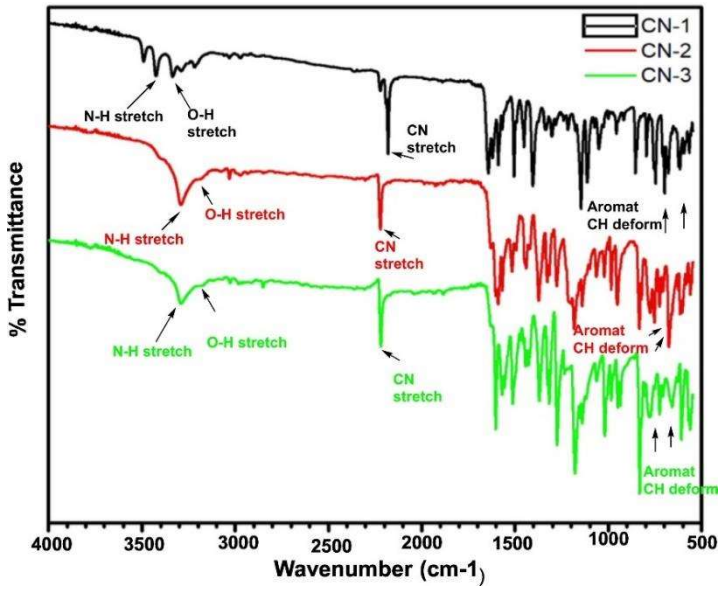

Figure 3.4 FTIR spectra of Naphthyridine derivatives

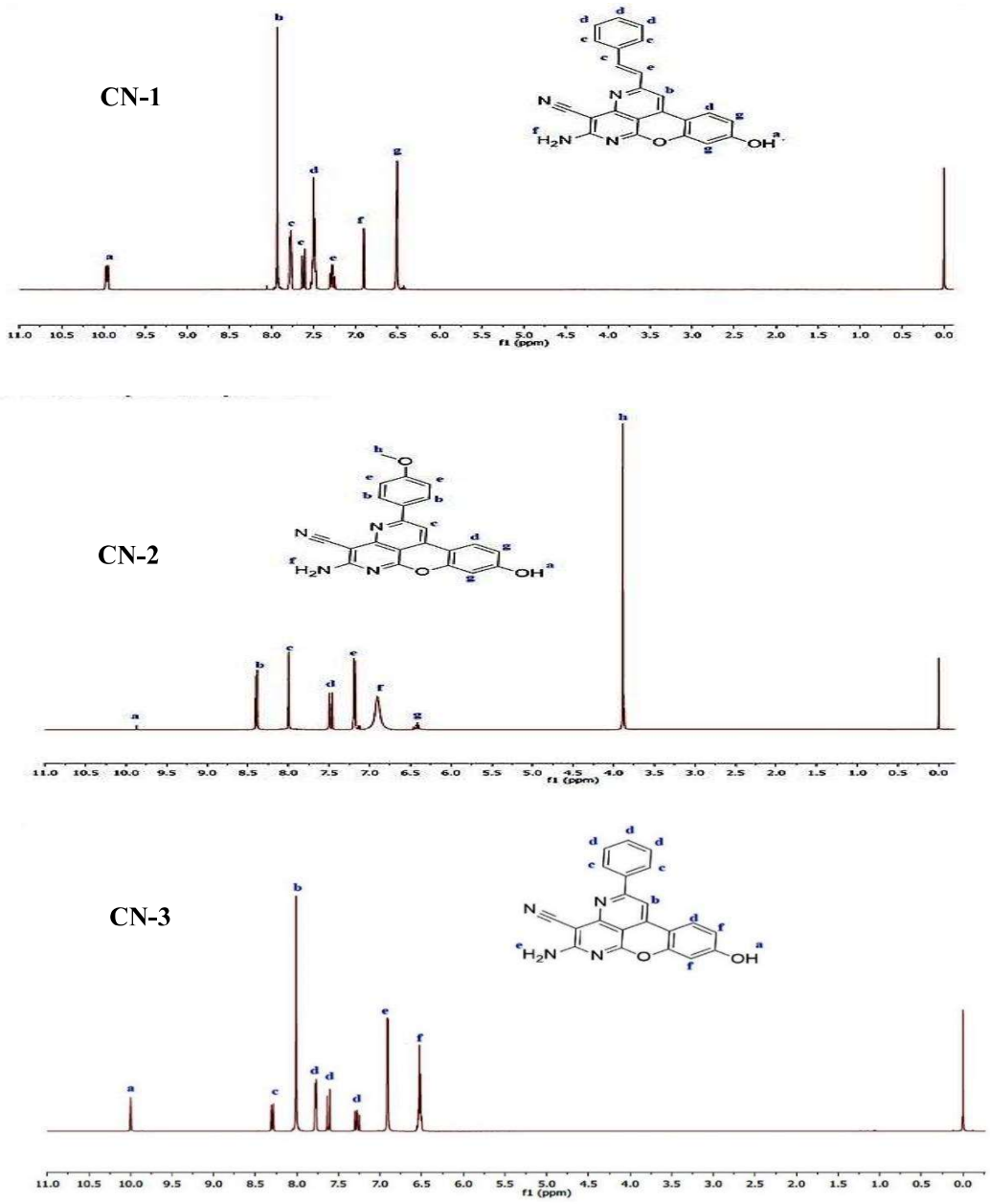

Figure 3.5 ^{1}H NMR spectra of Naphthyridine derivatives.

Table 3.5 The name, structure and characterization data of Naphthyridine derivatives inhibitors.

1.	5-amino-9-hydroxy-2-(4vinylphenyl)1,11b dihydro chromeno [4,3,2de] [1,6] naphthyridine 4-carbonitrile **(CN-1)**	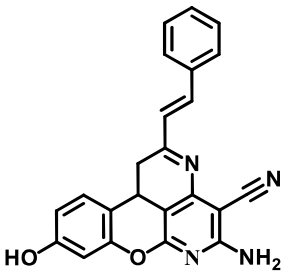	$C_{23}H_{18}N_4O_2$ (mol. wt.380.41). (M.P.>300°C **FTIR** (Vmax/ cm^{-1}) (KBr): 3331(NH str.), 3217 (OH str.), 3024 (aromatic CH str.), 2214 (CN str.), 1630 (aliphatic C=C str.), 1589, 1438 (aromatic ring str.), 1400, 1333 (amine CN str.), 1215, 1175, 1146, 1111, 1047, 998, 952, 915 (aromatic CH bend.), 854,793 (aromatic CH def.),695 (aromatic ring bend.)**^{1}H NMR** (500 MHz, DMSO-d6) δ (ppm) : 9.91 (OH), 7.91(Ar–H),7.67(Ar–H), 7.52 (Ar–H), 6.90 (−NH2), 6.49 (Ar–H), 7.31,7.61 (CH=CH),
2.	5-amino-9-hydroxy-2-(4-methoxyphenyl) chromeno[4,3,2-de] [1,6] naphthyridine-4-carbonitrile **(CN-2)**	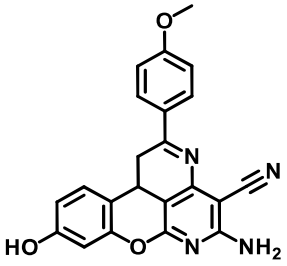	$C_{22}H_{16}N_4O_3$ (mol. wt.384.84). (M.P.>300°C); **FTIR** (Vmax/ cm^{-1}) (KBr): 3290 (NH str.), 3186 (OH str.), 3034 (aromatic CH str.), 2219 (CN str.), 1589, 1518, 1427 (aromatic ring str.), 1374, 1328 (amine CN str.), 1276, 1183 (C-O-C asymmetric str.), 831, 750 (C-O-C symmetric str.), 701 (aromatic CH def.), **^{1}H NMR** (500 MHz, DMSO-d6) δ (ppm): 9.87 (OH), 8.34 (Ar–H),7.98 (Ar–H), 7.45 (Ar–H), 7.21 (Ar–H), 6.87 (-NH_2), 6.44 (Ar–H), 3.86 (OCH_3).
3.	5-amino-9-hydroxy 2-phenyl chromeno[4,3,2-de][1,6]naphthyridine-4-carbonitrile **(CN-3)**	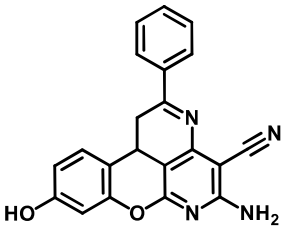	$C_{21}H_{14}N_4O_2$ (mol. wt.354.37). (M.P.>300°C); **FTIR** (Vmax/ cm^{-1}) (KBr): 3297(NH str.), 3186 (OH str.), 3032 (aromatic CH str.), 2226 (CN str.), 1589, 1569, 1438 (aromatic ring str.), 1368, 1319 (amine CN str.), 1277, 1180, 1146, 1062, 1016, 984, 946 (aromatic CH bend.), 834, 724 (aromatic CH def.), 660 (aromatic ring bend.). **^{1}H NMR** 500 MHz, DMSO-d6) δ (ppm): 9.98 (OH), 8.30 (Ar–H), 7.98 (Ar–H), 6.46 (Ar–H), 6.88 (-NH_2).

3.1.5.3. Synthesis of Hydroxyquinoline derivatives [(Ebenso, Obot, and Murulana 2010)]

A mixture of aromatic benzaldehyde (2 mmol), malononitrile (2 mmol), Resorcinol (2.5 mmol), and ammonium acetate (3 mmol) in water (6 ml) was refluxed for 5.0 h. After the reaction (TLC) was completed, the mixture was cooled and poured into crushed ice. The solid product was filtered to get an almost pure, crystallized product from ethanol. The outline for the synthesis is shown in scheme-3.3.

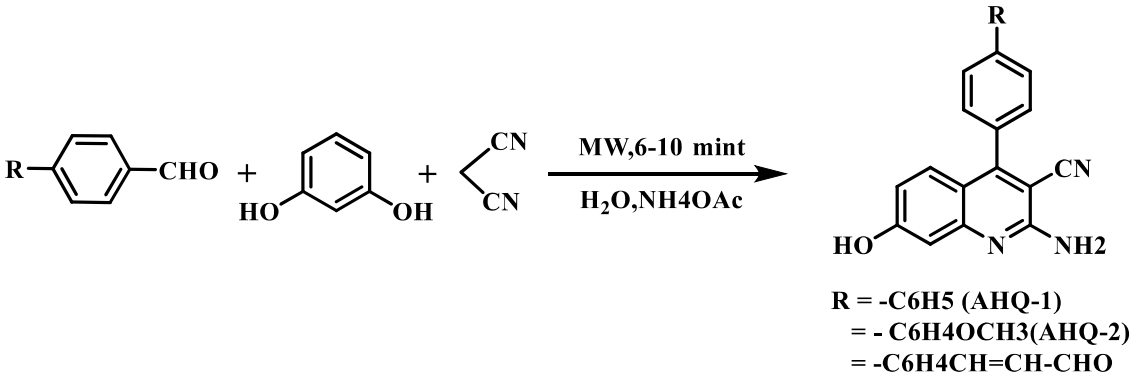

Scheme 3.3 Synthesis of Hydroxyquinoline derivatives

Table 3.6 The name, structure and characterization data of Hydroxy quinoline derivatives inhibitors.

S. No.	Name and Abbreviation of Inhibitor	Inhibitor structure	Characterization data
1.	2-Amino-7-hydroxy-4-phenylquinoline-3-carbonitrile **(AHQ-1).**	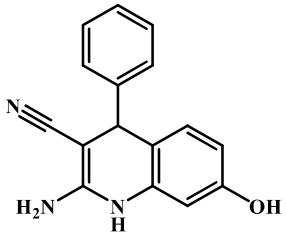	$C_{16}H_{33}N_3O$ (mol.wt. 263.30). (M.P 305°C **FTIR** (Vmax/ cm^{-1}) (KBr) : 3244 (–NH_2), 2916 (N–H), 2212 (–CN), 1641 (–C=C vinyl), 1585 (C=C aromatic). **Rf** = 0.69
2.	2-Amino-7-hydroxy-4-(4-methoxyphenyl) quinoline-3-carbonitrile **(AHQ-2)**	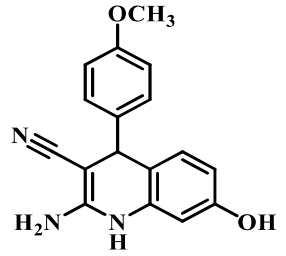	$C_{17}H_{15}N_3O_2$ (mol.wt. 293.33). (M.P.308°C); **FTIR** (Vmax/ cm^{-1}) (KBr):3241 (–NH_2), 2922 (N–H), 2213 (–CN),1631 (–C=C vinyl), 1578 (C=C aromatic). **Rf** = 0.73
3.	(E)-2-amino-7-hydroxy-4-styrylquinoline-carbonitrile **(AHQ-3**	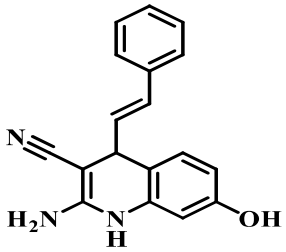	$C_{18}H_{15}N_3O$ (mol.wt. 289.30). (M.P.312°C); **FTIR (neat) ν (cm–1):** 3234 (–OH), 3329 (–NH_2), 2918 (N–H),2213 (–CN), 1624 (–C=C vinyl), 1565 (C=C aromatic). **Rf** = 0.76

3.1.5.4 Synthesis of substituted benzimidazole [(Zahed Karimi-Jaberi and Mohammad Amiri 2012)]

A mixture of aldehyde (2 mmol), *o*-phenylenediamine (2 mmol), boric acid (0.1 g) and water (1 mL) was stirred at room temperature for the appropriate time indicated in Table 1. The progress of reactions was monitored by TLC (ethyl acetate/petroleum ether=1/4). After completion of the reaction, water (5 mL) was added, and the, mixture was stirred for 10 min. The obtained solid was collected by filtration and purified by recrystallization from ethanol. The outline for the synthesis is shown in Scheme 3.4.

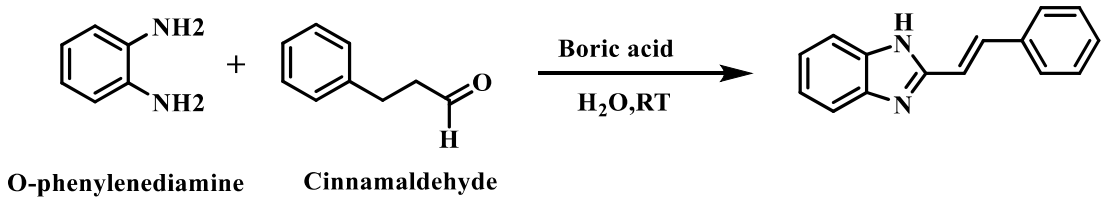

Scheme 3.4 Synthesis of substituted benzimidazole.

Table 3.7 The name, structure and characterization data of benzimidazole based inhibitors.

S. No.	Name and Abbreviation of Inhibitor	Inhibitor structure	Characterization data
1.	2-styryl-1H-benzo[d]imidazole **(STBim)**	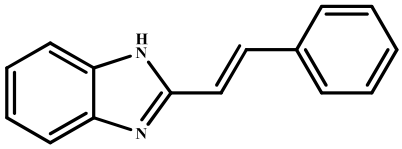	$C_{15}H_{12}N_2$ (mol. wt.263.30). (M.P 202°C **FTIR** (Vmax/ cm^{-1}) (KBr): 3376 (N–H stretch), 1590 (inplane N–H), 1365 (ring C–N), and 1259 (in-plane C–N) broad band around 3500 cm^{-1} **Rf** = 0.77

3.2 Equipment and Techniques Used

3.2.1. Characterization of the synthesized compounds

3.2.1.1 Determination of melting point: Melting points of the synthesized compounds were recorded on a Reichert Thermovar apparatus.

Determination of R_f values: R_f values were determined by thin layer chromatography using Silica-Gel G_{254} (MERCK) as support. N-Hexane and ethyl acetate were used in mobile phase in the respective ratio (6:1) as a developer.

Infrared spectroscopy: IR spectra were recorded by Jasco FT/IR-5300 spectrophotometer using KBr as an internal standard.

3.2.1.2 Determination of Corrosion Rate and Other related parameters

Weight Loss Method: The specimens of strip size (2.0 × 2.5 × 0.025 cm) of steel were mechanically abraded with 600-1200 grades of emery papers. In each specimen hole of 1.5 mm diameter was drilled to mount the specimen. After abrading, the specimens were washed with double distilled water and degreased with acetone, and finally dried in a hot air blower. After drying the specimens were placed in a desiccator and then used in an experiment. The cleaned and dried specimens were measured for the total surface area with utmost accuracy using the following equation [ASTM 1990, 3.02, G 31-72].

$$A = 2 (\text{length} \times \text{width} + \text{length} \times \text{thickness} + \text{width} \times \text{thickness} - \pi \times \text{radius}^2 + \pi \times \text{radius} \times \text{thickness}) \quad \text{---------- (3.1)}$$

The weight of the specimen has been measured before exposing it to the corrodent solution on an electronic balance. The volume of the test solution was kept 100 mL [(Mathur and Vasudevan 1982)] in all the experiments to avoid any appreciable change in its corrosivity during the test, either through exhaustion of corrosive constituent or by accumulate the ion of corrosion products that might affect further corrosion.The experiments were conducted under varied parameters of immersion time, solution, and inhibitor and acid temperature. The specimen was removed from the water after a predetermined amount of time and cleaned with running water. Any corrosion product on the steel surface has been manually removed using brush abrasion. After drying, the weight loss was measured by weighing the specimens.

The weight loss at desirable temperatures (1 K) was studied using a constant temperature thermostat. Using the following equations [ASTM 1987, 03-02, G1-72], the percentage inhibitory efficiency (IE%) was obtained.

$$\theta = \frac{C_R^0 - C_R^i}{C_R^0} \quad \text{---------- (3.2)}$$

$$IE\% = \frac{C_R^0 - C_R^i}{C_R^0} \times 100 \quad \text{---------- (3.3)}$$

Corrosion rate (C_R) in mmy^{-1} can be obtained by using the following equation:

$$C_R = \frac{87.6 \times w}{AtD} \quad \text{----- ---------- (3.4)}$$

where, w is the weight loss of the specimen (mg), A the surface area of specimen (cm^2), t the exposure time (h), and D the density of specimen ($g\ cm^{-3}$).

3.2.2 Electrochemical studies.

Gamry Instruments carried out electrochemical tests using three electrode assemblies. N80 and mild steels with an exposed area of 1 cm^2 are used as working electrodes. Counter and reference electrodes are made of graphite and saturated calomel, respectively. Steel was abraded with SiC sheets (up to 1200 grit) before each test, washed with acetone, and rinsed with double distilled water. To fit impedance data in an equivalent circuit and extrapolate

Tafel slopes, the GAMRY Echem Analyst software package 5.0 was utilised. Steel samples were immersed in corrosive for 30 minutes before each experiment, in the absence and presence of inhibitors, until a stable potential was achieved.

3.2.2.1 Electrochemical impedance spectroscopy.

Electrochemical Impedance measurements were carried out in frequency range from100 kHz to 0.5 Hz with amplitude of 10 mV peak to peak using AC signals vs open circuit potential.

The Nyquist and Bode plots of steel samples in the corrosive solution in absence and presence of inhibitors were obtained at 308 K. Different electrochemical parameters such as solution resistance (R_s), charge transfer resistance (R_{ct}), inductance (L) and CPE constants (Y_0 and n) was obtained by fitting using equivalent circuits. The impedance of the CPE can be given as follows [(Yadav, Quraishi, and Maiti 2012)].

$$Z_{CPE} = Y_0^{-1}(j\omega)^{-n} \tag{3.5}$$

where Y_0 is the amplitude comparable to a capacitance, j is the square root of -1, ω is angular frequency and n is the phase shift. The values of the double layer capacitance (C_{dl}) and inhibition efficiency (η %) are calculated as follow [D. K. Yadav *et al.* (2012)]:

$$C_{dl} = \frac{Y\omega^{n-1}}{\sin\left(n(\pi/2)\right)} \tag{3.6}$$

$$\eta\% = \left(1 - \frac{R_{ct}}{R_{ct(i)}}\right) \times 100 \qquad (3.7)$$

where, ω is the angular frequency (ω = 2π fmax) at which the imaginary part of impedance (-Zim) is maximal and n is the phase shift, R_{ct} and $R_{ct(i)}$ respectively represent the charge transfer resistance in absence and presence of inhibitors.

3.2.2.2 Potentiodynamic Polarization Technique:

Working electrode of size 1 × 1 cm (exposed) with a 7.5 cm long stem (isolated with commercially available lacquer, OPI PRODUCTSNSN: 853000N068480, Company's Name: OPI PRODUCTS INC) was cut from the steel and abraded with a series of 600 and 1200 emery papers. The specimens were. Then washed with distilled water, degreased with acetone, and dried in a hot air blower. After drying, the specimens were placed in a desiccator and used for an experiment. Potentiodynamic polarization studies were carried out using potentiostat/galvanostatostat (model G 300), with EIS software [ASTM 1991 G59-91]. A platinum foil of 1 × 1 cm and saturated calomel electrode were used as counter and reference electrodes, respectively. All the experiments were carried out at a constant temperature of 303 ± 1 K and a scan rate of 1.0 mV/sec for Tafel polarization and 0.125 mV/sec for linear polarization studies. The corrosion rate was calculated using the following relationship [ASTM 1994, 3.02, G 102-89].

$$C_R = \frac{0.13 \times i_{corr} \times E.W}{D} \quad \text{---------- (3.8)}$$

The percentage inhibition efficiency was calculated using the following equation:

$$IE\,\% = \frac{i^{0}_{corr} - i^{i}_{corr}}{i^{0}_{corr}} \times 100 \quad \text{---------- (3.9)}$$

Electrochemical Impedance Approach: In this technique, a three electrode assembly consisting of a mild steel strip as the working electrode, platinum as a counter electrode, and calomel as a reference electrode was used. The working electrode, or specimen, was abraded using emery paper ranging in grade from 600 to 1200, degreased with acetone, dried in a hot air blower, and kept in a desiccator. The mild steel strips were then dipped in the test solution and stored in the cell.The connecting of these electrodes is depicted in the circuit block diagram in Figure 3.6. After 15-20 minutes, the open circuit potential has stabilised.

Impedance measurements were performed at E_{corr} with the AC voltage amplitude + 10 mV in the frequency range from 100000 Hz to 0.01HzThe value of Rct was obtained using the Nyquist Plot [(Ashassi-Sorkhabi, Seifzadeh, and Hosseini 2008)]. The importance of solution resistance (R_s) is negligible for an acidic solution, and the R_s+R_{ct} values have been taken together as R_{ct}. The percentage inhibition efficiency was calculated using the following equation:

$$IE\% = \frac{R_{ct}^{i} - R_{ct}^{0}}{R_{ct}^{i}} \times 100 \quad \text{---------- (3.10)}$$

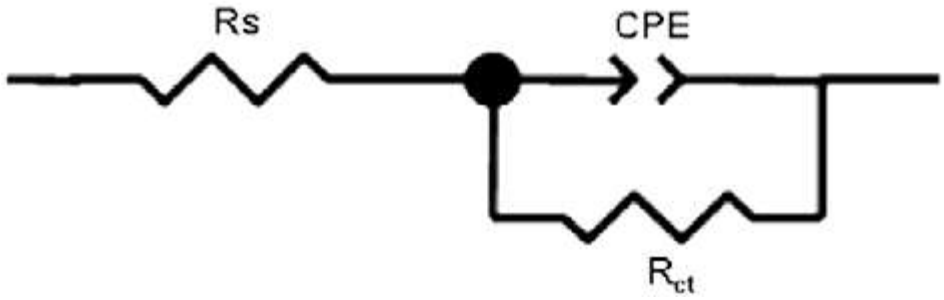

Figure 3.6 Block diagram of impedance set up including constant phase element.

In a simple circuit including a constant phase element, C_{dl} values have been calculated using the following equation:

$$C_{dl} = (Y_0 . R_{ct}^{1-n})^{1/n} \quad \text{---------- (3.11)}$$

Y_0 is the CPE constant, and n is a CPE exponent, which can determine the surface's heterogeneity or roughness.

3.2.3 Determination of Thermodynamics of Parameters.

3.2.3.1 (i) Determination of Activation Energy:

The corrosion rates were determined while maintaining all other parameters constant at temperatures ranging from 308 to 338 K. The activation energy (Ea) values were determined

using the Arrhenius equation from the slope of the log (CR) against 1/T plot(Khedr and Lashien 1992) [(Khedr and Lashien 1992)].

$$\log(C_R) = \frac{-E_a}{2.303RT} + \lambda \qquad \text{---------- (3.12)}$$

3.2.3.2 (ii) Determination of Enthalpy and Entropy of activation [(Abd El Rehim, Ibrahim, and Khalid 2001)]**:**

The other activation parameters, enthalpy, and entropy of activation were calculated from the slope and intercept of the plot log (C_R/T) *versus* $1/T$ using the equation:

$$C_R = \frac{RT}{Nh}\exp\left(\frac{\Delta S^*}{R}\right)\exp\left(-\frac{\Delta H^*}{RT}\right) \qquad \text{---------- (3.13)}$$

3.2.3.3 (iii) Determination of Free Energy of Adsorption:

The free energy of adsorption of inhibitor at the metal surface was calculated [Schorr *et.al.* (1972)] using the equation given below:

$$\Delta G^o_{ads} = -RT\ln(55.5K_{ads}) \qquad \text{---------- (3.14)}$$

And K_{ads} is given by:

$$K_{ads} = \frac{\theta}{1-\theta} \times \frac{1}{C_{inh}} \qquad \text{---------- (3.15)}$$

3.2.3.4 (iv) Determination of Enthalpy and Entropy of Adsorption: [Bouklah *et al.* (2006)]

The enthalpy and entropy of adsorption were calculated from the intercept and slope of the plot ΔG°_{ads} *versus* $1/T$ using the equation:

$$\Delta G^{\circ}_{ads} = \Delta H^{\circ}_{ads} - T\Delta S^{\circ}_{ads} \quad \text{---------- (3.16)}$$

3.2.4 Surface study

3.2.4.1 Scanning Electron Microscopy (SEM) study.

The surface morphology of the steel samples in absence and in presence of the inhibitors was studied by SEM. In this study the steel samples of dimension 5.0 cm× 2.5 cm× 0.2 cm were immersed in the corrosive solution in absence and presence of optimum concentration of inhibitors for 6h. After this the steel samples were taken out, washed with distilled water, dried and mechanically cut into 1cm^2 sizes for surface analysis. The instrument used is Ziess Evo 50 XVP instrument model, at an accelerating voltage of 5 kV and magnification 5kx.

3.2.4.2 Energy dispersive X-ray Spectroscopy (EDX) study.

The elemental composition of the deposited inhibitor coating on the steel surface was investigated using energy dispersive X-ray spectroscopy (EDX) in conjunction with scanning electron microscopy (SEM). The elements present on the steel surface before and after

exposure to the inhibitor solution were determined using EDX spectra. The equipment utilised is a Ziess Evo 50 XVP instrument model with a 5 kV accelerating voltage.

3.2.5 Theoretical study

3.2.5.1 Quantum chemical calculations.

DFT methods have been extensively used to perform quantum chemical calculations on the corrosion inhibition performance/purpose of many inhibitors. The DFT of Series 1 inhibitors carried out using Materials Studio software package (version 6.0) at DFT/GGA level using BOP functional and DNP basis set on all atoms [(Delley 1990; Al-Sabagh *et al*. 2015)]. The calculations were carried out after optimizing the structures. The COSMO [(Klamt and Schüürmann 1993)] controls were used for solvation effects (aqueous phase). While the DFTcalculations Series II, III and IV were performed using Gaussian 09 suite program [calculations were performed using Gaussian (2009)], on all the atoms using the B3LYP correlation functional and basis sets 3-21, 6-31G (d,p) and 6-311G (d,p) for Series II, Series III and Series IV, respectively . The corrosion testing is carried out in aqueous medium, therefore the DFT calculation of investigated inhibitors molecules was carried out in aqueous media and the effect of solvent on geometric and electronic parameters was modeled using integral equation formalism PCM (IEFPCM). After optimising the structures, the reactivity indices such as the energy of the highest occupied molecular orbital (E_{HOMO}) and the energy of the lowest unoccupied molecular orbital (E_{LUMO}) were computed. Other parameters such as energy gap (E), electronegativity (χ),

hardness (η) and softness (σ) and fraction of electron transfer (N) were calculated using E_{HOMO} and E_{LUMO} values using the following equations:

$$\Delta E = E_{LUMO} - E_{HOMO} \quad (3.17)$$

$$\eta = -1/2\ (E_{HOMO} - E_{LUMO}) \quad (3.18)$$

$$\sigma = 1/\eta \quad (3.19)$$

$$\chi = E_{LUMO} + E_{HOMO} \quad (3.20)$$

$$N = \frac{\phi - X_{inh}}{2(n_{Fe} - ni_{nh})} \quad (3.21)$$

3.2.5.2 Molecular dynamics simulation.

The most frequent method for studying the intermolecular interactions between corrosion inhibitor molecules and the metal surface under periodic boundary conditions is molecular dynamics (MD) simulation. [Hu *et al.* (2011), Yan *et al.* (2013)]. The Fe (110) surface with a slab of 5 was chosen for MD simulation in this study because it has a high stabilisation energy and a densely packed structure.The simulations were performed in a simulation box (24.8224.8235.69 3) that includes $9Cl^-$, $491H_2O$, $9H_3O^+$, and one inhibitor molecule to give a greater surface area for metal-inhibitor interactions. The simulations were built using the Visualizer, Amorphous Cell, and Discover modules from BIOVIA Materials Studio® commercial software [Accelrys (2013)]. MD simulations were run at

temperatures T = 303 K and T = 308 K kept constant by the Andersen thermostat, with a time step of 0.1 fs, NVT (fixed atom number, system volume, and temperature) ensemble, and a simulation length of 2000 ps to achieve an equilibrium state in the simulation system. Sun (1998) used the COMPASS (the Condensed-phase Optimized Molecular Potential for Atomistic Simulation Studies) force field to execute the energy minimization and MD calculation methods. The extent of the interactions of the inhibitor molecules adsorbed on Fe (110) surface can be demonstrated by their interaction ($E_{interaction}$)) and binding ($E_{binding}$) energies derived using Equations (3.22) and (3.23).

$$E_{interaction} = E_{total} - (E_{surface + solution} + E_{inhibitor}) \quad (3.22)$$

$$E_{Binding} = - E_{interaction} \quad (3.23)$$

where E_{total} represents the energy of the entire system, the $E_{surface + solution}$ denotes the entire energy of Fe (110) and the electrolytic solution in the absence of inhibitor molecules and $E_{inhibitor}$ denotes the whole energy of the inhibitor molecules.